doi:10.1111/j.1558-5646.2011.01558.x

JOINT RECONSTRUCTION OF DIVERGENCE TIMES AND LIFE-HISTORY EVOLUTION IN PLACENTAL MAMMALS USING A PHYLOGENETIC COVARIANCE MODEL

Nicolas Lartillot[1] and Frédéric Delsuc[2]

[1]*Département de Biochimie, Centre Robert-Cedergren pour la Bioinformatique, Université de Montréal, Québec H3T1J4, Canada*

E-mail: nicolas.lartillot@umontreal.ca

[2]*Institut des Sciences de l'Evolution, UMR5554-CNRS-IRD, Université Montpellier 2, 34095 Montpellier, France*

Received July 16, 2011
Accepted December 2, 2011
Data Archived: Dryad doi: 10.5061/dryad.tt28qk6f

Violation of the molecular clock has been amply documented, and is now routinely taken into account by molecular dating methods. Comparative analyses have revealed a systematic component in rate variation, relating it to the evolution of life-history traits, such as body size or generation time. Life-history evolution can be reconstructed using Brownian models. However, the resulting estimates are typically uncertain, and potentially sensitive to the underlying assumptions. As a way of obtaining more accurate ancestral trait and divergence time reconstructions, correlations between life-history traits and substitution rates could be used as an additional source of information. In this direction, a Bayesian framework for jointly reconstructing rates, traits, and dates was previously introduced. Here, we apply this model to a 17 protein-coding gene alignment for 73 placental taxa. Our analysis indicates that the coupling between molecules and life history can lead to a reevaluation of ancestral life-history profiles, in particular for groups displaying convergent evolution in body size. However, reconstructions are sensitive to fossil calibrations and to the Brownian assumption. Altogether, our analysis suggests that further integrating inference of rates and traits might be particularly useful for neontological macroevolutionary comparative studies.

KEY WORDS: **Ancestral reconstruction, Bayesian inference, comparative methods, independent contrasts, molecular clock.**

The hypothesis of the molecular clock has been an essential landmark in the history of evolutionary theory. The observation that sequence divergence among vertebrate globin genes appeared to be approximately proportional to divergence times (Zuckerkandl and Pauling 1962) has had several fundamental consequences, concerning the reconstruction of phylogenetic patterns, as well as the understanding of molecular evolutionary processes. On the phylogenetic side, the molecular clock opened the way to statistical methods for estimating divergence times based on molecular data. Since then, such methods have been extensively used to establish the chronology of evolution in various phylogenetic groups (reviewed in Bromham and Penny 2003; Benton and Donoghue 2007). On the molecular evolutionary side, the apparent regularity of the substitution process has played a key role in the selectionist versus neutralist debate, being used by Kimura as one of his key arguments in favor of the neutral theory of molecular evolution (Kimura 1983).

As genetic sequence data accumulated, however, it became progressively clearer that the molecular clock was at best an approximation. At virtually every phylogenetic scale, statistical tests have rejected a strict constancy of the substitution rate (Li and Tanimura 1987; Martin et al. 1992; Mooers and Harvey 1994; Lanfear et al. 2007; Lepage et al. 2007). Given the central role of the molecular clock in evolutionary studies, such a pervasive

violation raised several important issues. Among them, the question of what the determinants of rate variation might be, and how divergence times should be reconstructed in the absence of a strict molecular clock have attracted most of the attention.

Concerning the first question, the substitution rate appears to change in a genome-wide and systematic way (Lanfear et al. 2010), suggesting that a significant part of rate variation could be the consequence of changes in species life history, or in the parameters of the genetic system. Comparative analyses using independent contrast methods or related approaches (Felsenstein 1985; Martins and Hansen 1997; Paradis and Claude 2002; Garland et al. 2005; Lartillot and Poujol 2011) have provided many interesting insights in this direction. In mammals, which are the focus of the present article, the synonymous substitution rate was found to correlate with generation time (Li et al. 1996), or longevity (Welch et al. 2008) in the nuclear genome, and metabolic rate (Martin 1999), mass or longevity (Nabholz et al. 2008; Lartillot and Poujol 2011) in the mitochondrial genome. A positive correlation of dN/dS with body size in mitochondrial genomes (Popadin et al. 2007), or generation time in nuclear genomes (Nikolaev et al. 2007; Eyre-Walker et al. 2002), has been found, and interpreted in nearly neutral terms, that is, as a change in the strength of purifying selection due to changes in effective population size (Ohta 1973, 1995; Kimura 1979).

As for divergence time estimation, rate variation makes molecular dating methods considerably more complex, and potentially less reliable, than what they would have been under a strict clock. Given this problem, most of the work has consisted in phenomenological adaptations of the statistical framework, empirically accommodating different rates in different clades (Rambaut and Bromham 1998; Yoder and Yang 2000), or on each branch (Drummond et al. 2006), or modeling the instant rate of substitution as a Brownian diffusion (Thorne et al. 1998; Rannala and Yang 2007), or an Ornstein–Uhlenbeck process (Lepage et al. 2007). The resulting methods yield quite different results, compared to earlier findings based on the strict clock assumption. In particular, younger ancestors were found for groups such as mammals (Douzery et al. 2003; Hasegawa et al. 2003; Springer et al. 2003; Delsuc et al. 2004) or animals (Douzery et al. 2004; Peterson et al. 2008), compared to earlier estimates (Hedges et al. 1996; Wray et al. 1996), suggesting that relaxing the clock may partially reduce systematic biases in favor of old ages (Bromham and Hendy 2000). Nevertheless, molecular dating still needs improvement. Notably, the mechanistic basis of rate determination has never really been considered in the context of molecular dating. Mechanistic insights, however, could provide useful clues as to what type of stochastic process should be used for modeling the substitution rate. In addition, connections between rates and life-history traits may have a bearing on the cross-talk between paleontology and molecular data. If rate correlates with body size, then paleontological evidence about the trends in body-size evolution could be used to calibrate rate variation. For example, early mammals were probably smaller than extant ones (Kemp 2005), and thus, the rate of substitution might have been systematically higher in the deepest part of the mammalian tree. Failing to account for this phenomenon might contribute to make ancestors of placentals appear older than they actually are (Welch et al. 2008).

Correlations could also be used in the context of phylogenetic reconstruction of life history and morphological character evolution. Methods for reconstructing ancestral states of quantitative characters have been available for more than 20 years. First developed in a parsimony (Maddison 1991) or a least-square framework (McArdle and Rodrigo 1994), they have been reformulated using model-based statistical methods (Schluter et al. 1997; Martins and Hansen 1997). These statistical approaches typically use Brownian diffusion processes for describing character evolution, and are thus mathematically very similar to independent contrast methods and to relaxed clock models for estimating divergence times. Beyond the reconstruction of life-history profiles of specific ancestors along the phylogeny, general patterns of morphological and life-history evolution such as early-burst (Harmon et al. 2010), punctuated equilibria (Pagel et al. 2006; Mattila and Bokma 2008), balanced models (Butler and King 2004; Cooper and Purvis 2010), Cope's rule (Moen 2006; Monroe and Bokma 2010), or differential extinction as a function of body size (FitzJohn 2010), have motivated an extensive series of comparative analyses.

In practice, however, it has been observed that ancestral reconstruction is often highly uncertain (Schluter et al. 1997; Martins 1999; Webster and Purvis 2002), and increasingly so as one goes toward the root of the phylogenetic tree. It is also sensitive to the assumptions of the underlying model, in particular the undirected Brownian assumption (Oakley and Cunningham 2000; Webster and Purvis 2002). To compensate for the apparent lack of statistical power, one possibility would be to provide information about past character values using fossil data (Finarelli and Flynn 2006). However, such a strategy is not applicable to cases where the fossil record is poor, or where fossils are difficult to assign to particular lineages, as in the case of interorder relationships among placentals. Alternatively, information about ancestral life-history traits may be obtained via the correlation between life-history traits and the substitution rate. Ancestral substitution rates can in principle be reconstructed over the entire phylogeny. They are in fact a byproduct of the relaxed clock models used for estimating divergence times. Although ancestral rates are considered as nuisance parameters in the context of molecular dating, in a comparative perspective, they may turn out to represent a genuine source of phylogenetic information, increasing the statistical power of ancestral life-history trait reconstructions, and thus leading to more powerful tests of alternative scenarios of

morphological and life-history evolution. Neontological tests of Cope's rule (Moen 2006; Monroe and Bokma 2010), for instance, may obviously benefit from additional information about ancestral body size obtained via the correlation between body size and the substitution rate.

Altogether, some connections still need to be made between various questions bearing on molecular evolutionary mechanisms, divergence time estimation, comparative and morphological analyses. From a methodological point of view, in all cases, a very similar modeling framework is used, relying on Brownian-like diffusion processes to describe substitution rate variation or quantitative character evolution. This methodological kinship suggests that connections would be greatly facilitated by combining all these questions into a single modeling framework, broadly aimed at testing integrated macroevolutionary mechanisms and hypotheses. As a first step in this direction, a method for jointly estimating divergence times, substitution rates, life-history traits, and the correlations between them, was recently introduced (Lartillot and Poujol 2011). The estimation works by conditioning a probabilistic model simultaneously on a codon sequence alignment, a matrix of quantitative characters such as morphological data or life-history traits, and fossil calibrations. The framework is thus a fusion between classical codon models (Goldman and Yang 1994; Muse and Gaut 1994), autocorrelated relaxed clocks (Thorne et al. 1998; Rannala and Yang 2007), and comparative methods based on the idea of independent contrasts (Felsenstein 1985; Martins and Hansen 1997; Paradis and Claude 2002; Garland et al. 2005). It assumes allometrically correlated evolution of the rate of substitution and life-history traits, thus allowing estimation of the correlation between these variables. Simultaneously, the method marginally reconstructs divergence dates and life-history evolution, potentially relying on the correlations between rates and traits, and therefore, hopefully, leading to more accurate chronological and morphological estimates. Here, we apply this framework to a concatenation of 17 nuclear protein-coding genes in 73 placental taxa, and illustrate how it can be used to conduct joint inference of macroevolutionary patterns and processes in placental mammals. Our analysis, although being consistent with previous correlation studies and divergence time estimation, reveals that a joint modeling strategy might be particularly useful in the context of quantitative character reconstruction and macroevolutionary comparative studies.

Methods

We built upon the nuclear multigene datasets previously assembled for resolving the placental mammal phylogeny (Janecka et al. 2007; Miller-Butterworth et al. 2007; Springer et al. 2007). We downloaded from the Nucleotide database of GenBank at NCBI all mammalian sequences available for the following 17 single-copy protein-coding nuclear exons: ADORA3, ADRA2B, ADRB2, APOB, ATP7A, BDNF, BRCA1, CNR1, GHR, PNOC, RAG1, RAG2, RBP3 (ex-IRBP), S1PR1 (ex-EDG1), TYR, VWF, and ZFX. Three new xenarthran RBP3 sequences were obtained experimentally. Total genomic DNA was extracted from tissues preserved in 95% ethanol for *Myrmecophaga tridactyla*, *Tamandua tetradactyla*, and *Choloepus didactylus* using the QIAampDNA extraction kit (QIAGEN GmbH, Hilden, Germany). The RBP3 exon 1 was polymerase chain reaction (PCR) amplified in two overlapping fragments I1/J2 and I7/J1 using primers I1: 5'-ATGGCCAAGGTCCTCTTGGATAACTACTGCTT-3' (fwd), J2: 5'-CCACTGCCCTCCCATGTCTG-3' (rev), I7: 5'-CCCCTCCAACACGACCACNGAGATCTGG-3' (fwd), and J1: 5'-CGCAGGTCCATGATGAGGTGCTCCGTGTCCTG-3' (rev). PCR products were purified from 1% agarose gels using Amicon Ultrafree-DA columns (Millipore Corporation, Bedford, MA) and sequenced using the Big Dye Terminator cycle sequencing kit on an Applied ABI Prism 3130 XL automated sequencer. The new sequences have been deposited in the EMBL Nucleotide Sequence Database under accession numbers FR871851, FR871852, and FR871853. We then retrieved sequences of the same 17 exons from the 37 mammalian genomes available in the release 60 of EnsEMBL database. Finally, we selected 78 mammalian taxa for which at least nine of the 17 genes were available, including the platypus, four marsupials, and 73 placentals representing the widest phylogenetic diversity available to date with representatives from all existing orders. All sequences were trimmed to ensure that they started and ended with complete codons. Nucleotide sequences from each individual gene datasets were subsequently aligned based on their amino acid translation using a modified version of transAlign (Bininda-Emonds 2005) incorporating MAFFT (Katoh et al. 2005). Ambiguously aligned codons were then removed from each individual gene alignment using Gblocks (Castresana 2000) with default parameters. Visual inspection of maximum likelihood individual gene trees obtained using PhyML 3.0 with SPR moves (Guindon and Gascuel 2003) allowed excluding sequences corresponding to cases of obvious contaminations/misidentifications and of likely annotation errors in sequences from EnsEMBL. The 17 individual gene datasets were finally concatenated into a supermatrix totaling 15,117 nucleotide sites (i.e., 5039 codons). For the purpose of this work focusing on placentals, the supermatrix was reduced to the 73 placental taxa and contains only 17.48% of missing data. All sequence accession numbers are indicated in the Table S3. The two datasets have been deposited in the Dryad digital repository doi:10.5061/dryad.tt28qk6f.

The probabilistic framework for jointly estimating divergence times and life-history traits (introduced in Lartillot and Poujol 2011) is composed of three distinct components. First, the time-valued phylogenetic tree is assumed to be produced

by a homogeneous birth–death process with subsampling (Yang and Rannala 1997). Second, the rate of synonymous substitution (dS), the ratio of synonymous over nonsynonymous substitution (dN/dS), together with the three life-history traits considered in the present analysis (female age at maturity, body size, and maximum recorded life span), are allowed to vary among lineages in a correlated fashion, being represented by a multivariate Brownian diffusion process (of dimension 5) running along the branches of the phylogeny. This process is parameterized by a 5×5 covariance matrix Σ considered as unknown. Finally, the variation in dS and dN/dS along the phylogeny is integrated into a nonhomogeneous codon substitution process, based on the formalism of Muse and Gaut (1994). The model is conditioned on a multiple alignment and on a matrix of life-history traits, using fossil calibrations. A sample, approximately from the joint posterior distribution, is produced by Bayesian Markov chain Monte Carlo (MCMC), and is successively marginalized over three components of the model: covariance matrix, ancestral life-history reconstructions, and divergence times.

The topology we used reflects the classical multigene phylogenetic studies dividing placental mammals into four major groups (Madsen et al. 2001; Murphy et al. 2001a,b): Afrotheria (Springer et al. 2007), Xenarthra (Delsuc et al. 2002), Euarchontoglires (Huchon et al. 2002; Janecka et al. 2007; Blanga-Kanfi et al. 2009), and Laurasiatheria (Roca et al. 2004; Nishihara et al. 2006; Miller-Butterworth et al. 2007). Concerning the debated root of the placental tree, we favored Atlantogenata as supported by genome-scale analyses of indels distribution (Murphy et al. 2007). For calibrating the tree, we used the nine fossil constraints defined by Springer et al. (2003) to render the results as comparable as possible among studies. Information about three life-history traits was obtained from the AnAge database (de Magalhaes and Costa 2009). For each genus represented in the alignment, the logarithm of each trait was averaged over all species of the genus for which information was provided in AnAge. Independent analyses were run, in which, for each genus, the trait of the species representing the majority of the alignment was used. The results were very similar (compare Tables 1 and S2). Log-normality of life-history traits was assessed using the Shapiro–Wilk and D'Agostino's K-squared tests, applied to the independent contrasts. The independent contrasts were calculated based on the time-calibrated phylogeny obtained under the uncorrelated model (see below). None of the tests were rejected at the 0.05 level for any of the three life-history traits.

The following priors were used: on the covariance matrix, an inverse Wishart prior of parameter Σ_0 and with $M = 5$ degrees of freedom, where $\Sigma_0 = Diag(\kappa_1, \ldots, \kappa_M)$ is a diagonal matrix. For each $m = 1..M$, the prior on κ_m is a truncated Jeffrey's prior, on $[10^{-3}, 10^3]$ (which is equivalent to a uniform prior on $\ln \kappa_m$, restricted to the interval $[-3 \ln 10, 3 \ln 10]$). On divergence times, we imposed either a uniform prior, or a birth–death prior with parameters λ (birth rate), μ (death rate) and ω (sampling fraction at $t = 0$). To allow identifiability, and as in Rannala and Yang (2007), we set $p_1 = \lambda - \mu$ and $p_2 = \lambda\omega$. We impose an exponential prior of mean 10^{-3} on both p_1 and p_2 (with time being measured such that the root-to-tip distance is equal to 1).

The MCMC sampler was run for a total of 330,000 cycles, each cycle consisting of a complex series of MCMC updates over all variables of the model. The substitution mapping was resampled every 30 cycles, upon which a point was saved. The first 1000 points were discarded, and posterior averages were estimated on the remaining 10,000 points. Two independent runs were performed under each settings presented in this article. Convergence and mixing of the MCMC were first assessed visually, and then quantified using convergence diagnostics previously introduced (Lartillot et al. 2009). These diagnostics consist in measuring the overlap between the credibility intervals obtained from the two independent runs, and estimating the decorrelation time and the effective sample size for several key statistics (the log likelihood, the total length of the tree, the average dN/dS, all entries of the covariance matrix, and the age of the root). For all these summary statistics, and with a true sample size of 10,000 points, effective sample size was always larger than 500, and the overlap between credibility intervals was always greater than 95%,

Partial correlation analyses were performed using the precision matrix, which is the inverse of the covariance matrix: $\Omega = \Sigma^{-1}$ (Dempster 1972). For each i, j, $i \neq j$, $-\Omega_{ij}$ is equal to the partial covariance between variables i and j (i.e., controlling for all other variables). The partial correlation coefficients are

Table 1. Covariance analysis.

Marginal correlations[1]	dN/dS	Maturity	Mass	Longevity
dS	−0.07	−0.55**	−0.60**	−0.64**
dN/dS	–	0.36**	0.07	0.27*
Maturity	–	–	0.62**	0.69**
Mass	–	–	–	0.74**
Partial correlations[2]	dN/dS	Maturity	Mass	Longevity
dS	0.16	−0.20	−0.16	−0.29*
dN/dS	–	0.33*	−0.25	0.22
Maturity	–	–	0.24*	0.27*
Mass	–	–	–	0.50**

[1]Correlation coefficients corresponding to the marginal correlations between each pair of variables.
[2]Correlation coefficients corresponding to the partial correlations.
*Posterior probability of a positive correlation < 0.05 or > 0.95.
**Posterior probability of a positive correlation < 0.025 or > 0.975.

given by Wong et al. (2003):

$$r_{ij} = -\frac{\Omega_{ij}}{\sqrt{\Omega_{ii}\Omega_{jj}}}.$$

Partial correlation coefficients were computed for, and averaged over, each point of the sample obtained by MCMC, and the posterior probability of a positive (or a negative) partial correlation was estimated as the fraction of such points for which the partial correlation was positive (or negative).

To evaluate the significance of global trends, the sum of branch-wise independent contrasts was used as the test statistic (the sign of this sum tends to reflect the direction of the global trend.) To simulate replicates from the posterior predictive distribution, each point of the sample obtained by MCMC was taken in turn. Based on the divergence times and the covariance matrix defined by this point, a simulation of the multivariate Brownian diffusion process was done, and the test statistic was recomputed on this realization. The number of times the value of the statistic computed on a posterior predictive replicate was larger (in the case of dS) or smaller (in the case of life-history traits) than the observed value, which was taken as our estimates of posterior-predictive P-values.

Results and Discussion

CORRELATION ANALYSIS

Although the focus of the present article is on life-history reconstruction and divergence times estimation, we briefly comment on the estimated covariance matrix (Table 1). We observe a strong and significant negative correlation between the synonymous substitution rate and all three life-history traits. Multiple regression (see Methods) indicates that the correlation is essentially between synonymous substitution rate and maximum life span (correlation coefficient $r = -0.29$, posterior probability of a negative covariance $pp = 0.96$ when controlling for age at maturity and mass). Mass and female age at maturity are only indirectly correlated with dS, via their positive correlation with longevity. Inspection of the branch-wise independent contrasts (Lartillot and Poujol 2011) associated to the terminal branches of the phylogeny indicates that human maximum life span is an outlier. The correlations, however, are robust to the removal of the human longevity, and also, to the extreme adult body masses of the whale *Megaderma*, the elephant *Loxodonta*, and the rhinoceros *Ceratotherium* (Table S1). These results are broadly in accordance with previously published correlation analyses (Speakman 2005; Lanfear et al. 2007; Nabholz et al. 2008; Welch et al. 2008).

Concerning nonsynonymous substitutions, we find a significant positive correlation of dN/dS with age at maturity ($r = 0.36$, $pp = 0.98$, Table 1), which remains significant ($pp = 0.96$) when controlling for other variables, including the synonymous substitution rate. This positive correlation could be interpreted as an indirect negative correlation between dN/dS and population size, that is, a stronger purifying selection in species with larger population sizes (Ohta 1995; Eyre-Walker et al. 2002; Nikolaev et al. 2007). Note, however, that no correlation is seen, even marginally, between dN/dS and body mass ($r = 0.07$, $pp = 0.68$), in spite of the fact that body size is probably also correlated with population size in mammals. In contrast, dN/dS displays a positive correlation primarily with body mass in mitochondrial proteins (Popadin et al. 2007; Lartillot and Poujol 2011). The reasons for this discrepancy between the nuclear and mitochondrial compartments are not clear, and will need to be further investigated.

THE EVOLUTION OF LIFE HISTORY

The joint reconstruction of divergence times and life-history evolution obtained under the phylogenetic covariance model is summarized for a few key ancestral nodes in Table 2, and graphically displayed on Figure 1 for the case of body mass (age at maturity and maximum life span in Figs. S1 and S2). Although the covariance analysis of the last section indicates that maximum life span is more directly correlated with substitution rates than substitution rate is with body size, the marginal correlation between the synonymous substitution rate and body size remains nevertheless strong and significant ($r^2 = 35\%$, Table 1). The focus of the present section is therefore on body size, as it can more easily be discussed in the context of paleontological evidence.

The most recent common ancestor of placentals is inferred to be a rather small animal (mode 1 kg, 95% credibility interval: 0.4–10.7 kg), although perhaps not as small as what would have been expected based on the overall size distribution of therian fossils of the Cretaceous (more in the range of 10–800 g, Alroy 1999). The female age at maturity of this ancestor is estimated to be between 208 and 824 days, and its longevity between 11 and 25 years. According to the reconstruction, body mass starts to increase early on in the Cretaceous, by 70 Myr in the lineages leading to afrotherians and xenarthrans, and 90 Myr in the ancestors of cetartiodactyls and ferungulates. After the Cretaceous-Tertiary (KT) boundary, the increase in body size is more apparent, in particular in cetartiodatyls, perissodactyls, proboscideans, and anthropoid primates. Other lineages, such as chiropterans or elephant shrews, show a marked decrease of body size during their evolution, whereas other lineages such as rodents seem to have remained stable in size. The overall uncertainty in the reconstruction of all three life-history traits is large, however (Figs. 1 and 2; Table 2).

The life-history evolution reconstructed by the present method is a combination of two sources of information. First, the correlation between rates and traits is implicitly used by the model to convert information about rates into information about ancestral traits. Second, the continuity property of the Brownian

Table 2. Estimates (95% credibility intervals) of ancestral life-history traits for several ancestral nodes.

	Mass (kilograms)		Age at maturity (days)		Longevity (years)	
	Cov[1]	Uncorr[2]	Cov[1]	Uncorr[2]	Cov[1]	Uncorr[2]
Placentalia	(0.2, 8.7)	(0.4, 15.6)	(208, 824)	(226, 956)	(11, 25)	(12, 29)
Afrotheria	(0.5, 29.5)	(0.7, 47.1)	(212, 792)	(234, 1146)	(13, 31)	(13, 36)
Xenarthra	(0.2, 30.1)	(0.3, 45.4)	(192, 1042)	(200, 1230)	(12, 34)	(13, 39)
Laurasiatheria	(0.4, 10.7)	(0.6, 15.8)	(259, 831)	(260, 955)	(12, 25)	(12, 27)
Eulipotyphla	(0.1, 6.0)	(0.2, 9.1)	(211, 894)	(196, 997)	(9, 21)	(9, 24)
Perissodactyla	(5.5, 587.8)	(6.1, 822.9)	(337, 1867)	(350, 2086)	(17, 46)	(17, 45)
Chiroptera	(0.01, 1.1)	(0.01, 1.0)	(245, 1111)	(195, 1044)	(13, 32)	(17, 45)
Ferae	(0.7, 28.8)	(0.9, 47.6)	(257, 1053)	(262, 1294)	(13, 29)	(13, 34)
Carnivora	(0.8, 77.6)	(1.5, 163.3)	(236, 1261)	(281, 1594)	(12, 32)	(13, 39)
Cetartiodactyla	(0.9, 64.0)	(7.7, 499.4)	(174, 763)	(320, 1477)	(11, 27)	(17, 44)
Cetruminantia	(2.4, 173.9)	(23.5, 1435.8)	(212, 981)	(394, 1754)	(13, 32)	(20, 52)
Whippomorpha	(6.0, 376.1)	(32.3, 2086.1)	(274, 1228)	(423, 1976)	(16, 39)	(22, 57)
Euarchontoglires	(0.2, 4.3)	(0.2, 6.0)	(221, 737)	(211, 784)	(11, 22)	(11, 24)
Glires	(0.1, 3.9)	(0.1, 5.4)	(201, 705)	(185, 749)	(10, 20)	(9, 22)
Euarchonta	(0.2, 4.8)	(0.2, 6.0)	(220, 763)	(210, 802)	(11, 23)	(11, 25)
Simiiformes	(0.2, 14.4)	(0.3, 31.1)	(383, 1906)	(408, 2134)	(16, 41)	(17, 48)
Catarrhini	(0.6, 35.4)	(1.4, 71.7)	(578, 2408)	(708, 3018)	(21, 50)	(24, 60)

[1]Credibility intervals obtained under the covariant model.
[2]Credibility intervals obtained under the uncorrelated model.

process smoothes out the overall reconstruction, such that nearby nodes tend to display similar life-history profiles. The Brownian assumption can be seen as the application of a path-minimizing penalization on life-history reconstruction. In the present probabilistic context, and as in previously proposed maximum likelihood methods (Martins and Hansen 1997; Schluter et al. 1997), this minimization is enforced in a more elastic way than in a least-square framework (Maddison 1991; McArdle and Rodrigo 1994). Nevertheless, it amounts to a parsimony criterion, minimizing convergent evolution or reversion given the constraints otherwise imposed by the data.

To get a more precise idea of the interplay between these multiple sources of information and constraints, we reconstructed life-history evolution under a version of the model obtained by setting the nondiagonal entries of the covariance matrix to zero (Lartillot and Poujol 2011). This uncorrelated model only relies on the continuity property of the Brownian motion, and is thus conceptually very close to methods proposed previously (Martins and Hansen 1997; Schluter et al. 1997), also relying on Brownian models to describe the evolution of quantitative characters. Although we do not provide any quantitative assessment of the relative fit of the two models, covariant and uncorrelated, it can be noted that the two models are nested, and therefore, the significant correlation found among life-history traits and substitution rates (Table 1) is in itself a good qualitative indication that the covariant model fits the data better than the uncorrelated one.

The two estimates obtained under the covariant and the uncorrelated models are displayed in Table 2 and Figure 2 for several nodes of interest (see also Figs. S3– S5). Overall, the two reconstructions yield similar results. However, there are several important exceptions, in particular, in carnivores, anthropoid primates (Simiiformes), and cetartiodactyls. In the three clades, the body size estimated for the ancestor and its immediate descendants are smaller under the covariant model than under the uncorrelated settings. In anthropoids and carnivores, the difference is about twofold, whereas in cetartiodactyls, up to a 10-fold reduction of body size is observed for the ancestor of Whippomorpha (hippos + cetaceans), and of Cetruminantia (ruminants + whippomorphs, Table 2), although in all cases, the overlap between credibility intervals remains large (always more than 50%, Fig. 2).

This result can be interpreted as follows. At least in the case of anthropoid primates and cetartiodactyls, these two groups are exclusively composed of large animals. Anthropoid primates also have a long generation time, compared to other placentals. Since the assumption that body size follows an undirected Brownian motion makes convergent evolution a priori unlikely, without any additional information, it is more parsimonious for the uncorrelated model to infer that the successive ancestors in each group were also large. On the other hand, the substitution patterns inferred along the phylogeny contain a signal in favor of high rates of substitutions in the early lineages of the two groups,

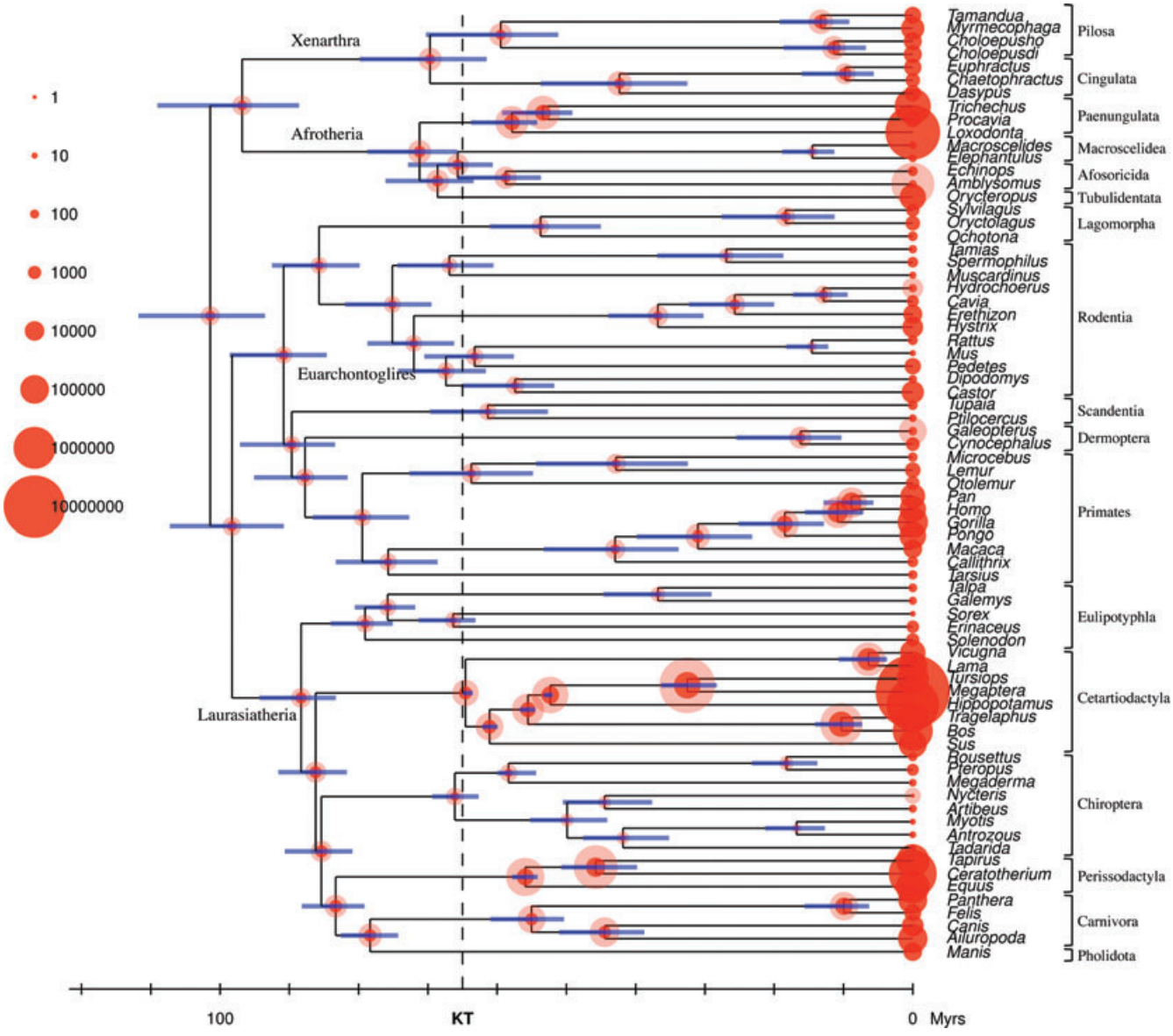

Figure 1. **Joint reconstruction of divergence times and adult body mass (in grams) under the covariant model. Horizontal bars indicate 95% credibiity intervals for node ages. Dark- and light-shaded disks indicate 95% credibility intervals for ancestral body masses. In the case of extant taxa for which body size was missing, credibility intervals are reconstructed as for internal nodes.**

suggesting that body size might have been smaller in the ancestors. Integrating this information, the covariant model reevaluates the ancestral body sizes downwards, thus making a compromise between the correlation signal and the Brownian assumption, and acknowledging a pattern of convergent evolution toward larger body size in both groups.

In the case of anthropoid primates, the difference between the two models is sensitive to the presence of human longevity. Without human longevity, the trend toward smaller ancestral body masses under the covariant model is still observed, although it now represents a difference of approximately 30% (Table S4). The case of carnivores is also not totally clear, as the extant species of the group span a large diversity of adult body sizes. However, the smallest species of the order (e.g., herpestids and mustelids) are not represented in our dataset. In addition, perissodactyls, the sister group of carnivores and pangolins, is composed of large animals (horses, rhinos, and tapirs). These two factors may jointly contribute to the large ancestral body size inferred by the uncorrelated model, an inference which is corrected downwards once substitution rates are considered. For most other groups, body size is not fundamentally different between the covariant and the uncorrelated models, although there is a slight downward reevaluation in many cases, once rates are considered (e.g., perissodactyls, afrotherians, and xenarthrans, Table 2).

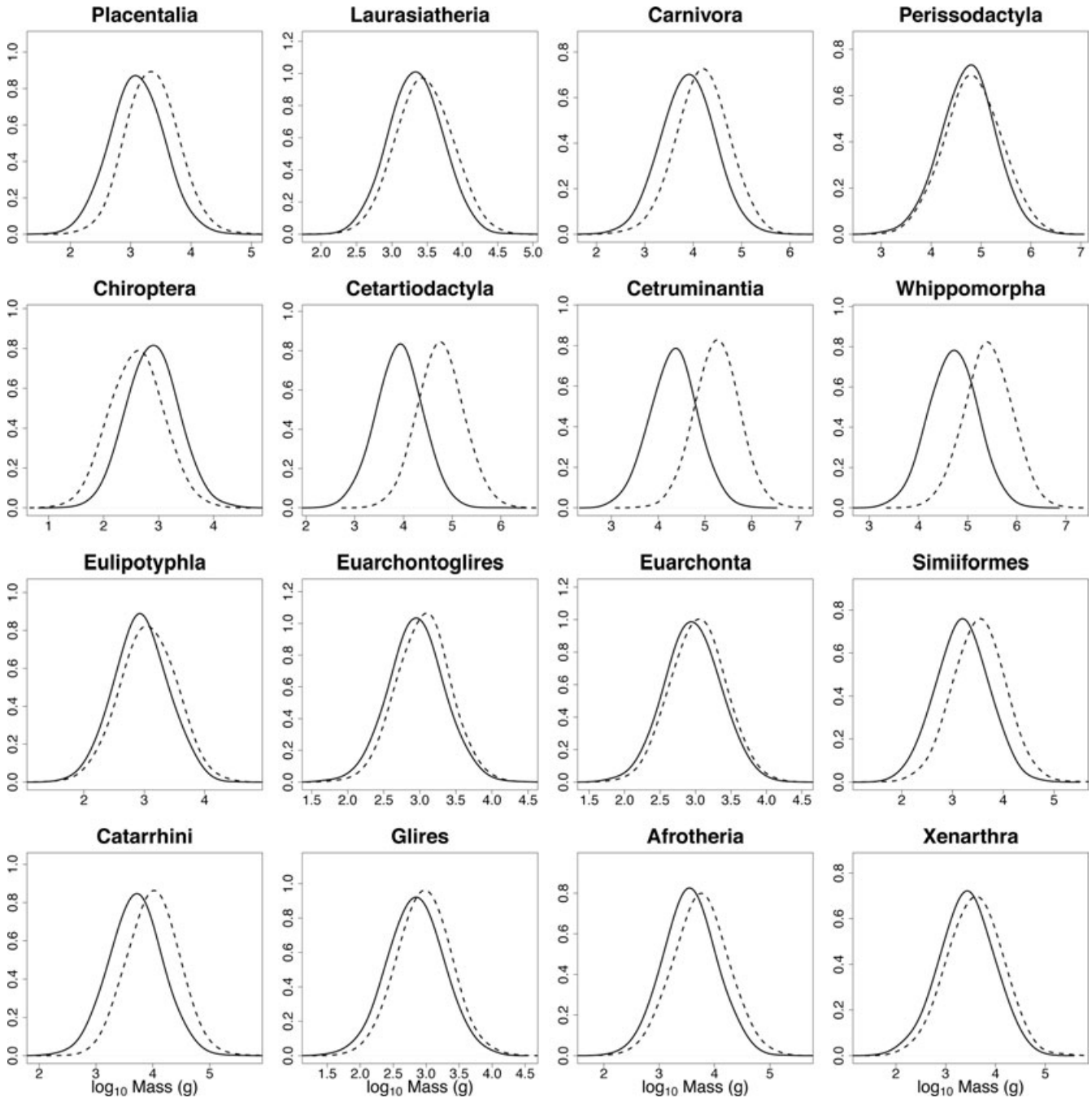

Figure 2. **Posterior distribution on ancestral body mass for several ancestors. Solid lines indicate covariant model. Dashed lines indicate uncorrelated model.**

Interestingly, cetartiodactyls are one of the few groups on which an upper time constraint (< 65 Myr) has been imposed (following Springer et al. 2003). This upper bound is exerting a strong constraint on the analysis, and contributes to the convergent evolution pattern inferred at the base of the group. Without the constraint, the ancestral body sizes estimated under the covariant model are more similar to those obtained under the uncorrelated model. For instance, the adult body mass of the last common ancestor of cetruminantia is only two to three times smaller than under the uncorrelated model, compared to the 10-fold reduction observed in the presence of the upper calibration (Figs. 3 and S6). On the other hand, without the upper constraint, the cetartiodactyl divergence is shifted back into the Cretaceous (95 % credibility interval: 65.9–73.3 Myr), and the placentals are also significantly older, by approximately 10 Myr (95 % credibility interval: 99–118 Myr, Fig. S6). Apart from this important difference, the overall reconstruction is not sensitive to changes in fossil calibrations, and in particular, is very similar whether the calibrations of

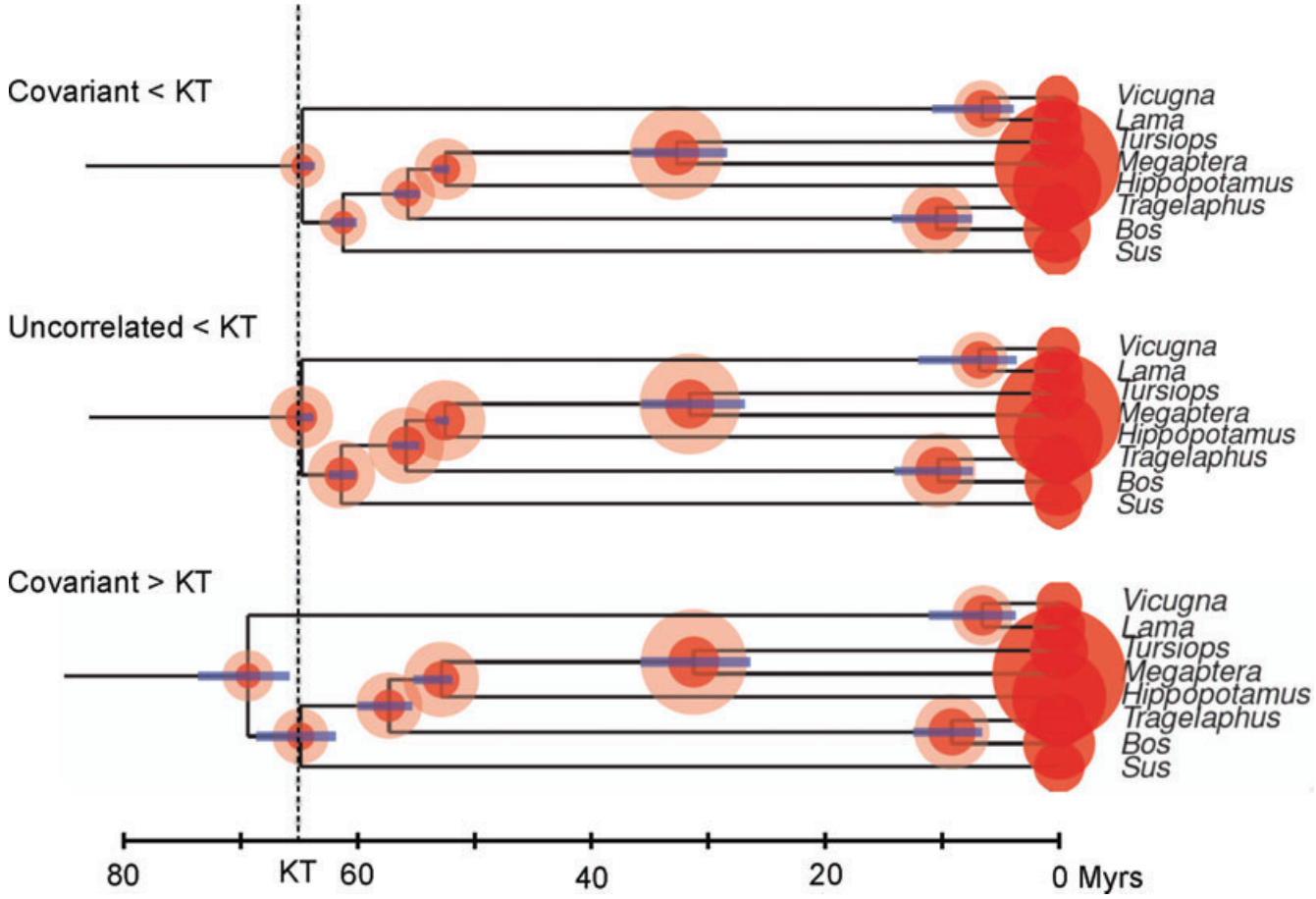

Figure 3. Joint reconstruction of divergence times and adult body mass (in grams) in cetartiodactyls, under the covariant model (top), uncorrelated model (middle), and covariant model without the upper constraint on the order (bottom). Horizontal bars indicate 95% credibiity intervals for node ages. Dark- and light-shaded disks indicate 95% credibility intervals for ancestral body masses.

Springer et al. (2003) or those proposed by Benton et al. (2009) are used (Fig. S8).

Cetartiodactyls therefore represent an interesting case where a complex interplay between fossil calibration, rates, traits, and divergence times, is taking place, and for which there are at least two possible interpretations. On one hand, the upper calibration on cetartiodactyls could be incorrect. Upper constraints are notoriously difficult to justifiy (Benton et al. 2009), and this particular one is even more subject to discussion, in a context where a long-fuse scenario (Archibald and Deutschman 2001) of post-KT intraorder diversification is not necessarily taken for granted. On the other hand, the body sizes inferred for cetartiodactyls under the covariant model are perhaps more reasonable with the calibration than without (Fig. 3), and are more in agreement with fossils. Known early cetaceans were probably small, about the size of a wolf for *Himalayacetus* and *Pakicetus*, or even of a fox in the case of *Ichtyolestes* (Thewissen et al. 2001). Thus, an alternative interpretation would be that the divergence times and the body masses inferred under the covariant model, and using the upper constraint of 65 Myr for cetartiodactyls, would be fundamentally correct. In contrast, the old age found for the ancestor of the order without the upper bound, the conflict between the reconstructed evolution of body mass under the uncorrelated and the fully covariant models, and the similar pattern observed in anthropoid primates and carnivores, would all represent indications of a violation of the undirected Brownian assumption.

GLOBAL TRENDS IN MOLECULAR AND LIFE-HISTORY EVOLUTION

Convergent evolution toward low substitution rate and large body size (and other life-history traits) seems to more globally prevail over the whole placental tree (Fig. 4, black squares). That the model infers the trend on life-history traits via their correlations with molecular substitution parameters is indicated by the absence of any trend on traits when this correlation is suppressed, that is, under the uncorrelated model (Fig. 4, white circles). Note that, in terms of the underlying mechanism, the trend most probably occurs primarily at the level of life-history evolution, and translates only secondarily into a downward trend on the substitution rate. In terms of estimation, however, the situation is reversed.

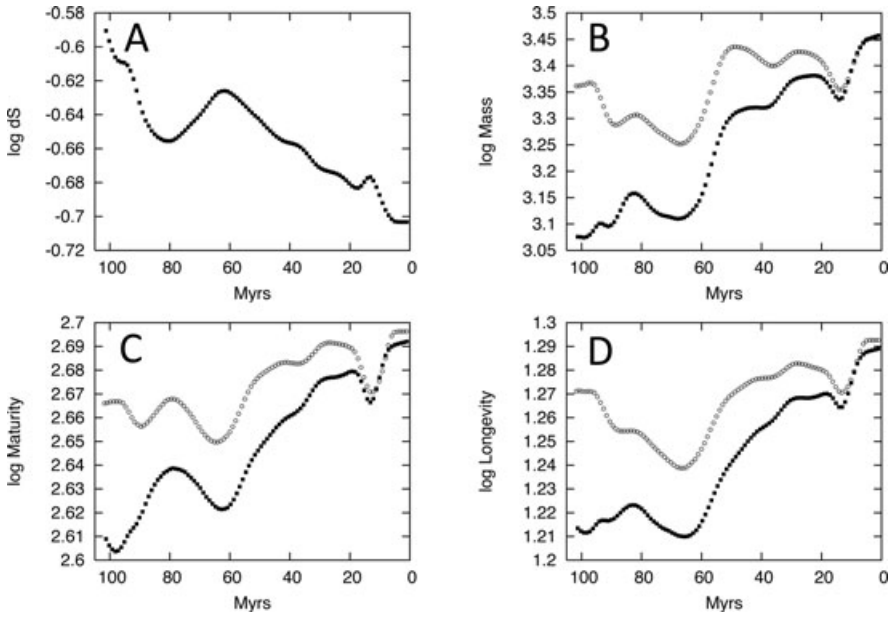

Figure 4. Timeline along the placental phylogeny of (A) substitution rate, (B) mass, (C) age at maturity, and (D) longevity. In B, C, and D, black squares indicate covariant model and white circles indicate uncorrelated model.

Via the sequence alignment, it is the substitution rate that contains information about ancient trends, that are then interpreted in terms of life-history evolution by the model, via the covariance matrix.

The trends are not significant using a posterior predictive test (posterior predictive P-value $P = 0.10$, for a negative trend in the substitution rate, $P = 0.36$, 0.22, and 0.29 for a positive trend on age at maturity, mass, and longevity, see Methods). However, this could be due to the fact that the undirected Brownian motion opposes an excessive rigidity to the modulations provided by rate–trait correlations. This importantly suggests that, ultimately, the global trends should be explicitly integrated into the modeling framework, and estimated along with the covariance matrix and divergence times.

Interestingly, the increase in body size spans the entire Cenozoic, and is not restricted to the period immediately following the KT boundary. A sharp increase in mean log body mass right after KT is supported by paleontological data, possibly as a result of the ecological release experienced by placentals following the extinction of nonavian dinosaurs (Alroy 1999, 1998). However, this increase is mostly due to groups since then extinct (Smith et al. 2010). Here, in contrast, the lineages displayed in Figure 1 are those that gave rise to modern placental species, and may not be representative of all lineages existing at a given geological time instant. In particular, if large-bodied species are more prone to extinction (Clauset and Erwin 2008; FitzJohn 2010), the ancestors of extant taxa are expected to be on average smaller than their contemporaries. The trend observed in placental body-size evolution (Fig. 4) could therefore be interpreted as an instance of Cope's or Stanley's rule (Stanley 1973), either the result of an intralineage adaptive trend toward larger body size, or a retrospective species-selection effect created by the higher rate of extinction of larger-bodied species.

INFERRED DIVERGENCE TIMES

Globally, divergence times (Fig. 1) are similar to those obtained by previous analyses using Bayesian Brownian relaxed clocks (Hasegawa et al. 2003; Springer et al. 2003; Delsuc et al. 2004; Murphy et al. 2007). In particular, the age of the ancestor of placentals is estimated at around 100 Myr (credibility interval from 93 to 113 Myr). Several orders originate and diversify before the KT boundary, thus following a short-fuse scenario (primates, insectivores, and rodents), whereas all other orders conform to a long-fuse pattern, with Cretaceous origins and subsequent diversification in the Tertiary (in the case of cetartiodactyls, by virtue of an a priori constraint). The estimation was robust to the choice of the prior on divergence (birth–death prior in Fig. 1, vs. uniform prior in Fig. S7).

Comparing divergence times estimated by the uncorrelated and the covariant model reveals one local difference, however, in catarrhinian primates (Table 3). Specifically, the successive nodes along the lineage leading from humans to their last common ancestor with macaques are all older by about 2–3 Myr. A reasonable interpretation of this finding is that the long generation times of extant primates are taken by the covariant model as indirect evidence of low substitution rates in the clade. As a result, the deconvolution of rate and time performed by the model on the observed sequence divergence is shifted toward longer

Table 3. Estimates (95% credibility intervals) of divergence times in catarrhinian primates.

	Age (million years)			
	With human longevity		Without human longevity	
	Cov[1]	Uncorr[2]	Cov[1]	Uncorr[2]
Homo Pan	(5.7, 12.8)	(4.3, 10.2)	(3.8, 8.7)	(3.1, 8.3)
Homo Gorilla	(7.1, 15.4)	(5.4, 12.6)	(5.0, 10.5)	(4.1, 10.3)
Homo Pongo	(12.7, 25.0)	(10.7, 22.3)	(9.6, 21.2)	(8.6, 19.2)
Homo Macaca	(23.1, 39.9)	(21.2, 38.4)	(18.7, 36.3)	(18.1, 34.3)

[1]Credibility intervals obtained under the covariant model.
[2]Credibility intervals obtained under the uncorrelated model.

times and smaller rates, compared to what is done under the uncorrelated model. These observations are consistent with the existence of a possible systematic bias on divergence dates due to convergent evolution toward larger body size (Welch et al. 2008), although we did not observe such effects at a more global scale. In particular the age of the last common ancestor of all placentals inferred by the two models is virtually the same (between 93 and 112 Myr under the covariant model, vs. 92–113 Myr under the uncorrelated model).

Of note, the difference between the two models concerning divergence times in catarrhinians is less pronounced in the absence of information about human longevity (Table 3). The overall younger ages found without human longevity, both under the covariant and the uncorrelated models, also suggest that the extreme variation in longevity along the terminal branch leading to humans has itself an influence on divergence times estimation, presumably requiring more time to be accounted for under a regular Brownian motion.

Perspectives

Seen in a long-term perspective, the approach adopted here defines the broad lines of a general framework assigning a well-defined place to each type of macroevolutionary question. In this framework, molecular evolutionary mechanisms are represented by the correlation structure between rates and traits. Diversification scenarios are fundamentally priors on divergence times. Macroevolutionary hypotheses define the general shape of the process of trait evolution along the phylogeny. Whichever question is the focus of one's interest, in all cases, the problem reduces to estimating parameters or measuring the fit of the joint model, by simultaneously conditioning on morphological, molecular, and paleontological data. Specific questions are finally answered by obtaining the relevant marginals. To what extent joint estimation of all these components will empower empirical macroevolutionary studies remains to be determined, but the present analysis already provides several suggestions in this respect.

Concerning correlations between rates and traits, our observations (Table 1) are not fundamentally different from what has been obtained using less-integrated methods (Li et al. 1996; Welch et al. 2008; Nikolaev et al. 2007). This suggests that the independent contrast method is qualitatively robust to uncertainties and violations of the underlying assumptions. The main advantage of the present formalism, however, will probably appear more clearly once more complex correlation analyses, involving other aspects of the substitution process, have been implemented. Also, it is more easily amenable to explicit mechanistic developments, while accounting for correlations with life-history traits across the phylogeny.

Whether phylogenetic covariance is important for divergence time estimation is also not totally clear. At first sight (Fig. 1), integrating a relaxed molecular clock with life-history covariation does not seem to fundamentally change the estimation of divergence dates. However, in the analyses presented here, the only constraint about life-history traits has been provided at the leaves of the tree, for extant species. In some cases, in particular for cetartiodactyls, we retrospectively compared reconstructed ancestral body sizes with known fossils, but in principle, fossils could be used to directly enforce constraints on ancestral body sizes, in the hope that those constraints would inform divergence time estimation (Welch et al. 2008). To do this, however, information about fossils should not be included as constraints directly applied to ancestral nodes, as has been done here. Instead, fossils should be represented as true taxa in the phylogeny, constrained to stand at the time corresponding to their geological strata. The situation is analogous to serial samples of viral populations (as in Drummond et al. 2006), and should be dealt with in a similar way. Once this is done, information about fossil body size can be naturally included, exactly as for extant taxa. Finally, time-dependent distributions of body size estimated from fossils could also be used to calibrate the process of life-history evolution in a more global fashion, possibly using methods such as those developed by FitzJohn (2010) to account for differential extinction as a function of body size.

Regardless of the impact of the joint modeling strategy on estimated dates, the observations gathered here cast a new light on important issues concerning divergence time estimation. For instance, the fact that body size explains up to 35% of the variation in the substitution rate, combined with the observation that entire orders are either small (e.g., rodents) or large (e.g., cetartiodactyls), clearly points to the existence of pervasive rate autocorrelation across branches. Thus far, however, such considerations have been virtually absent from the debate about whether rate variation is best modeled using autocorrelated or nonautocorrelated models in divergence time estimation methods (Ho et al. 2005; Drummond et al. 2006; Lepage et al. 2007; Battistuzzi et al. 2010; Linder et al. 2011). Conversely, the violation of the Brownian

assumption indicated by our analysis of body-size evolution in placentals, combined with the knowledge that substitution rate and body size are strongly correlated, suggests that the Brownian assumption may also be violated in the case of substitution rates. Clearly, a promising approach to improving divergence date estimation will be to model departures from the Brownian motion while relying on explicit process-based connections between rate and life-history evolution.

Concerning ancestral reconstruction of quantitative characters, from simulations and real applications, it has already been observed that such reconstructions are both uncertain and potentially sensitive to violations of the Brownian assumption (Schluter et al. 1997; Martins 1999). In particular, it was found, using experimental evolution of viruses, that ancestral reconstruction using a Brownian model is particularly inadequate in the face of convergent evolution (Oakley and Cunningham 2000). Similarly, convergent evolution is the most likely explanation for the discrepancy observed here between the uncorrelated and the covariant models in the cases of cetartiodactyls and primates (Table 2), and thus, our observations confirm the inadequacy of Brownian motions to accomodate convergent evolution. Interestingly, in the present case, the comparison between inference with and without information from substitution rates offers an internal test of the adequacy of the Brownian motion.

Altogether, it is certainly difficult to offer a definitive interpretation of the observations presented in this analysis from a macroevolutionary perspective. Even if our interpretation of the discrepancies observed between the covariant and the uncorrelated models is correct, such discrepancies fundamentally point to model violation problems. Nevertheless, from a methodological standpoint, all these phenomena are interesting as they illustrate the intricate interplay between rates, dates, and traits, while again emphasizing the potential role of violations of the Brownian assumption in the context of divergence time estimation and life-history reconstruction, a necessary step before moving to more adequate modeling strategies.

It may have been hoped that relying on the additional information provided by the correlation between life-history traits and substitution parameters would have allowed the inference to overcome the limitations of the underlying model of character evolution, and would have resulted in more robust ancestral inference. Yet, the credibility intervals obtained under the covariant model are not narrower than (and significantly overlap with) the intervals obtained under the uncorrelated model, clearly suggesting that the correlation between dS and body size is not sufficiently strong to significantly reduce the uncertainty. In the long term, other aspects of the substitution patterns across the tree will probably be found to correlate with life-history variables, and therefore, one could imagine that combining a large array of such correlations would ultimately result in increasingly precise estimation of ancestral life-history profiles. Focussing on substitution parameters depending only on the relative substitution rates, and not the absolute rate, might also have the advantage of providing molecular correlates of life-history variation less dependent on the complex entanglement between rates and dates, and thus more robust against uncertainties about fossil calibrations and divergence times estimation.

On the other hand, even if correlations between rates and traits turn out to be too weak to ever permit reliable inference about the life-history profile of specific ancestors taken in isolation, testing hypotheses about global macroevolutionary patterns is probably the type of question for which the present approach is most promising. Inference about global patterns, such as bursts or trends at the scale of the group as a whole (Harmon et al. 2010; Monroe and Bokma 2010), integrates the information over the entire phylogeny. In this context, joint inference of rates and traits, using models that would explicitly relax the Brownian assumption, for instance, by allowing for parameter-dependent systematic trends along the lineages, could provide much additional statistical power. Testing alternative macroevolutionary scenarios then becomes a model comparison question, allowing one to test hypotheses about the presence of directed change or more general global effects across the phylogeny. How such global patterns would impact the estimated correlations between rates and life-history characters, or the estimated divergence times, is an open question, which clearly needs further investigation.

Similarly, hypotheses about diversification patterns can in principle be formalized in the present context. However, this should be done using complete phylogenies, unlike what has been done here. To do this, one possibility would be to embed the tree spanned by the taxa present in the multiple alignment into a larger phylogenetic tree, possibly accounting for incomplete information about the topology (as in FitzJohn et al. 2009). Doing this would avoid the data and taxon selection problems potentially raised by the present analysis, while opening new possibilities in terms of integrative hypothesis testing of correlations between diversification patterns, molecular evolution, and life-history evolution.

ACKNOWLEDGMENTS

We wish to thank N. Rodrigue, H. Philippe, and two anonymous reviewers for their useful comments on the manuscript. Computational resources were provided by Calcul Québec and Compute Canada. NL was funded by the Natural Science and Engineering Research Council of Canada, and by the Canadian Foundation for Innovation. FD acknowledges financial support from the Centre National de la Recherche Scientifique (PEPS-INSB-2010), and the Scientific Council of Université Montpellier 2 (CS-UM2-2010). Data used in this work were partly produced through technical facilities of the SFR Montpellier Environnement Biodiversité and phylogenetic analyses benefited from the ISEM computing cluster. This is contribution ISEM 2011-156 of the Institut des Sciences de l'Evolution de Montpellier (UMR 5554-CNRS-IRD).

LITERATURE CITED

Alroy, J. 1998. Cope's rule and the dynamics of body mass evolution in North American fossil mammals. Science 280:731–734.

———. 1999. The fossil record of North American mammals: evidence for a Paleocene evolutionary radiation. Syst. Biol. 48:107–118.

Archibald, J. D., and D. H. Deutschman. 2001. Quantitative analysis of the timing of the origin and diversification of extant placental orders. J. Mammal. Evol. 8:107–124.

Battistuzzi, F. U., A. Filipski, S. B. Hedges, and S. Kumar. 2010. Performance of relaxed-clock methods in estimating evolutionary divergence times and their credibility intervals. Mol. Biol. Evol. 27:1289–1300.

Benton, M. J., and P. C. J. Donoghue. 2007. Paleontological evidence to date the tree of life. Mol. Biol. Evol. 24:26–53.

Benton, M., P. Donoghue, and R. Asher. 2009. Calibrating and constraining molecular clocks. Pp. 35–86 *in* The timetree of life. Oxford Univ. Press, Oxford.

Bininda Emonds, O. R. P. 2005. transAlign: using amino acids to facilitate the multiple alignment of protein-coding DNA sequences. BMC Bioinform. 6:156.

Blanga-Kanfi, S., H. Miranda, O. Penn, T. Pupko, R. W. DeBry, and D. Huchon. 2009. Rodent phylogeny revised: analysis of six nuclear genes from all major rodent clades. BMC Evol. Biol. 9:71.

Bromham, L. D., and M. D. Hendy. 2000. Can fast early rates reconcile molecular dates with the Cambrian explosion? Proc. Biol. Sci. 267:1041–1047.

Bromham, L., and D. Penny. 2003. The modern molecular clock. Nat. Rev. Genet. 4:216–224.

Butler, M. A., and A. A. King. 2004. Phylogenetic comparative analysis: a modeling approach for adaptive evolution. Am. Nat. 164:683–695.

Castresana, J. 2000. Selection of conserved blocks from multiple alignments for their use in phylogenetic analysis. Mol. Biol. Evol. 17:540–552.

Clauset, A., and D. H. Erwin. 2008. The evolution and distribution of species body size. Science 321:399–401.

Cooper, N., and A. Purvis. 2010. Body size evolution in mammals: complexity in tempo and mode. Am. Nat. 175:727–738.

Delsuc, F., M. Scally, O. Madsen, M. J. Stanhope, W. W. de Jong, F. M. Catzeflis, M. S. Springer, and E. J. P. Douzery. 2002. Molecular phylogeny of living xenarthrans and the impact of character and taxon sampling on the placental tree rooting. Mol. Biol. Evol. 19:1656–1671.

Delsuc, F., S. F. Vizcaíno, and E. J. P. Douzery. 2004. Influence of tertiary paleoenvironmental changes on the diversification of South American mammals: a relaxed molecular clock study within xenarthrans. BMC Evol. Biol. 4:11.

Dempster, A. 1972. Covariance selection. Biometrics 28:157–175.

Douzery, E. J. P., F. Delsuc, M. J. Stanhope, and D. Huchon. 2003. Local molecular clocks in three nuclear genes: divergence times for rodents and other mammals and incompatibility among fossil calibrations. J. Mol. Evol. 57(Suppl. 1):S201–S213.

Douzery, E. J. P., E. A. Snell, E. Bapteste, F. Delsuc, and H. Philippe. 2004. The timing of eukaryotic evolution: does a relaxed molecular clock reconcile proteins and fossils? Proc. Natl. Acad. Sci. USA 101: 15386–15391.

Drummond, A. J., S. Y. W. Ho, M. J. Phillips, and A. Rambaut. 2006. Relaxed phylogenetics and dating with confidence. PLoS Biol. 4:e88.

Eyre-Walker, A., P. D. Keightley, N. G. C. Smith, and D. Gaffney. 2002. Quantifying the slightly deleterious mutation model of molecular evolution. Mol. Biol. Evol. 19:2142–2149.

Felsenstein, J. 1985. Phylogenies and the comparative method. Am. Nat. 125:1–15.

Finarelli, J. A., and J. J. Flynn. 2006. Ancestral state reconstruction of body size in the Caniformia (Carnivora, Mammalia): the effects of incorporating data from the fossil record. Syst. Biol. 55:301–313.

FitzJohn, R. G. 2010. Quantitative traits and diversification. Syst. Biol. 59:619–633.

FitzJohn, R. G., W. P. Maddison, and S. P. Otto. 2009. Estimating trait-dependent speciation and extinction rates from incompletely resolved phylogenies. Syst. Biol. 58:595–611.

Garland, T., Jr, A. F. Bennett, and E. L. Rezende. 2005. Phylogenetic approaches in comparative physiology. J. Exp. Biol. 208:3015–3035.

Goldman, N., and Z. Yang. 1994. A codon-based model of nucleotide substitution for protein-coding DNA sequences. Mol. Biol. Evol. 11: 725–736.

Guindon, S., and O. Gascuel. 2003. A simple, fast, and accurate algorithm to estimate large phylogenies by maximum likelihood. Syst. Biol. 52:696–704.

Harmon, L. J., J. B. Losos, T. J. Davies, R. G. Gillespie, J. L. Gittleman, W. B. Jennings, K. H. Kozak, M. A. McPeek, F. Moreno-Roark, T. J. Near, et al. 2010. Early bursts of body size and shape evolution are rare in comparative data. Evolution 64:2385–2396.

Hasegawa, M., J. L. Thorne, and H. Kishino. 2003. Time scale of eutherian evolution estimated without assuming a constant rate of molecular evolution. Genes Genet. Syst. 78:267–283.

Hedges, S. B., P. H. Parker, C. G. Sibley, and S. Kumar. 1996. Continental breakup and the ordinal diversification of birds and mammals. Nature 381:226–229.

Ho, S. Y. W., M. J. Phillips, A. J. Drummond, and A. Cooper. 2005. Accuracy of rate estimation using relaxed-clock models with a critical focus on the early metazoan radiation. Mol. Biol. Evol. 22:1355–1363.

Huchon, D., O. Madsen, M. J. J. B. Sibbald, K. Ament, M. J. Stanhope, F. Catzeflis, W. W. de Jong, and E. J. P. Douzery. 2002. Rodent phylogeny and a timescale for the evolution of glires: evidence from an extensive taxon sampling using three nuclear genes. Mol. Biol. Evol. 19:1053–1065.

Janecka, J. E., W. Miller, T. H. Pringle, F. Wiens, A. Zitzmann, K. M. Helgen, M. S. Springer, and W. J. Murphy. 2007. Molecular and genomic data identify the closest living relative of primates. Science 318:792–794.

Katoh, K., K. I. Kuma, T. Miyata, and H. Toh. 2005. Improvement in the accuracy of multiple sequence alignment program MAFFT. Genome Inform. 16:22–33.

Kemp, T. S. 2005. The origin and evolution of mammals. Oxford Univ. Press, Oxford.

Kimura, M. 1979. Model of effectively neutral mutations in which selective constraint is incorporated. Proc. Natl. Acad. Sci. USA 76:3440–3444.

———. 1983. The neutral theory of molecular evolution. Cambridge Univ. Press, Cambridge.

Lanfear, R., J. A. Thomas, J. J. Welch, T. Brey, and L. Bromham. 2007. Metabolic rate does not calibrate the molecular clock. Proc. Natl. Acad. Sci. USA 104:15388–15393.

Lanfear, R., J. J. Welch, and L. Bromham. 2010. Watching the clock: studying variation in rates of molecular evolution between species. Trends Ecol. Evol. 25:495–503.

Lartillot, N., T. Lepage, and S. Blanquart. 2009. Phylobayes 3: a Bayesian software package for phylogenetic reconstruction and molecular dating. Bioinformatics 25:2286–2288.

Lartillot, N., and R. Poujol. 2011. A phylogenetic model for investigating correlated evolution of substitution rates and continuous phenotypic characters. Mol. Biol. Evol. 28:729–744.

Lepage, T., D. Bryant, H. Philippe, and N. Lartillot. 2007. A general comparison of relaxed molecular clock models. Mol. Biol. Evol. 24: 2669–2680.

Li, W., D. Ellsworth, J. Krushkal, B. Chang, and D. Hewett-Emmett. 1996. Rates of nucleotide substitution in primates and rodents and the generation-time effect hypothesis. Mol. Phylogenet. Evol. 5:182–187.

Li, W.-H., and M. Tanimura. 1987. The molecular clock runs more slowly in man than in apes and monkeys. Nature 326:93–96.

Linder, M., T. Britton, and B. Sennblad. 2011. Evaluation of Bayesian models of substitution rate evolution–parental guidance versus mutual independence. Syst. Biol. 60:329–342.

Maddison, W. 1991. Squared-change parsimony reconstructions of ancestral states for continuous-valued characters on a phylogenetic tree. Syst. Biol. 40:304–314.

Madsen, O., M. Scally, C. J. Douady, D. J. Kao, R. W. DeBry, R. Adkins, H. M. Amrine, M. J. Stanhope, W. W. de Jong, and M. S. Springer. 2001. Parallel adaptive radiations in two major clades of placental mammals. Nature 409:610–614.

de Magalhaes, J. P., and J. Costa. 2009. A database of vertebrate longevity records and their relation to other life-history traits. J. Evol. Biol. 22:1770–1774.

Martin, A. P. 1999. Substitution rates of organelle and nuclear genes in sharks: implicating metabolic rate (again). Mol. Biol. Evol. 16:996–1002.

Martin, A. P., G. J. Naylor, and S. R. Palumbi. 1992. Rates of mitochondrial DNA evolution in sharks are slow compared with mammals. Nature 357:153–155.

Martins, E. 1999. Estimation of ancestral states of continuous characters: a computer simulation study. Syst. Biol. 48:642–650.

Martins, E. P., and T. F. Hansen. 1997. Phylogenies and the comparative method: a general approach to incorporating phylogenetic information into the analysis of interspecific data. Am. Nat. 149:646–667.

Mattila, T. M., and F. Bokma. 2008. Extant mammal body masses suggest punctuated equilibrium. Proc. Biol. Sci. 275:2195–2199.

McArdle, B., and A. Rodrigo. 1994. Estimating the ancestral states of a continuous-valued character using squared-change parsimony: an analytical solution. Syst. Biol. 43:573–578.

Miller-Butterworth, C. M., W. J. Murphy, S. J. O'Brien, D. S. Jacobs, M. S. Springer, and E. C. Teeling. 2007. A family matter: conclusive resolution of the taxonomic position of the long-fingered bats, Miniopterus. Mol. Biol. Evol. 24:1553–1561.

Moen, D. S. 2006. Cope's rule in cryptodiran turtles: do the body sizes of extant species reflect a trend of phyletic size increase? J. Evol. Biol. 19:1210–1221.

Monroe, M. J., and F. Bokma. 2010. Little evidence for Cope's rule from Bayesian phylogenetic analysis of extant mammals. J. Evol. Biol. 23:2017–2021.

Mooers, A. O., and P. H. Harvey. 1994. Metabolic rate, generation time, and the rate of molecular evolution in birds. Mol. Phylogenet. Evol. 3:344–350.

Murphy, W., E. Eizirik, W. Johnson, Y. Zhang, O. Ryder, and S. O'Brien. 2001a. Molecular phylogenetics and the origins of placental mammals. Nature 409:614–618.

Murphy, W. J., E. Eizirik, S. J. O'Brien, O. Madsen, M. Scally, C. J. Douady, E. Teeling, O. A. Ryder, M. J. Stanhope, W. W. de Jong, et al. 2001b. Resolution of the early placental mammal radiation using Bayesian phylogenetics. Science 294:2348–2351.

Murphy, W. J., T. H. Pringle, T. A. Crider, M. S. Springer, and W. Miller. 2007. Using genomic data to unravel the root of the placental mammal phylogeny. Genome Res. 17:413–421.

Muse, S. V., and B. S. Gaut. 1994. A likelihood approach for comparing synonymous and nonsynonymous nucleotide substitutions, with applications to chloroplast genome. Mol. Biol. Evol. 11:715–724.

Nabholz, B., S. Glémin, and N. Galtier. 2008. Strong variations of mitochondrial mutation rate across mammals—the longevity hypothesis. Mol. Biol. Evol. 25:120–130.

Nikolaev, S. I., J. I. Montoya-Burgos, K. Popadin, L. Parand, E. H. Margulies, National Institutes of Health Intramural Sequencing Center Comparative Sequencing Program, and S. E. Antonarakis. 2007. Life-history traits drive the evolutionary rates of mammalian coding and noncoding genomic elements. Proc. Natl. Acad. Sci. USA 104:20443–20448.

Nishihara, H., M. Hasegawa, and N. Okada. 2006. Pegasoferae, an unexpected mammalian clade revealed by tracking ancient retroposon insertions. Proc. Natl. Acad. Sci. USA 103:9929–9934.

Oakley, T. H., and C. W. Cunningham. 2000. Independent contrasts succeed where ancestor reconstruction fails in a known bacteriophage phylogeny. Evolution 54:397–405.

Ohta, T. 1973. Slightly deleterious mutant substitutions in evolution. Nature 252:315–354.

Ohta, T. 1995. Synonymous and nonsynonymous substitutions in mammalian genes and the nearly neutral theory. J. Mol. Evol. 40:56–63.

Pagel, M., C. Venditti, and A. Meade. 2006. Large punctuational contribution of speciation to evolutionary divergence at the molecular level. Science 314:119–121.

Paradis, E., and J. Claude. 2002. Analysis of comparative data using generalized estimating equations. J. Theor. Biol. 218:175–185.

Peterson, K. J., J. A. Cotton, J. G. Gehling, and D. Pisani. 2008. The Ediacaran emergence of bilaterians: congruence between the genetic and the geological fossil records. Philos. Trans. R. Soc. Lond. B Biol. Sci. 363:1435–1443.

Popadin, K., L. V. Polishchuk, L. Mamirova, D. Knorre, and K. Gunbin. 2007. Accumulation of sightly deleterious mutations in mitochondrial protein-coding genes of large versus small mammals. Proc. Natl. Acad. Sci. USA 104:13390–13395.

Rambaut, A., and L. Bromham. 1998. Estimating divergence dates from molecular sequences. Mol. Biol. Evol. 15:442–448.

Rannala, B., and Z. Yang. 2007. Inferring speciation times under an episodic molecular clock. Syst. Biol. 56:453–466.

Roca, A. L., G. K. Bar-Gal, E. Eizirik, K. M. Helgen, R. Maria, M. S. Springer, S. J. O'Brien, and W. J. Murphy. 2004. Mesozoic origin for West Indian insectivores. Nature 429:649–651.

Schluter, D., T. Price, A. Mooers, and D. Ludwig. 1997. Likelihood of ancestor states in adaptive radiation. Evolution 51:1699–1711.

Smith, F. A., A. G. Boyer, J. H. Brown, D. P. Costa, T. Dayan, S. K. M. Ernest, A. R. Evans, M. Fortelius, J. L. Gittleman, M. J. Hamilton, et al. 2010. The evolution of maximum body size of terrestrial mammals. Science 330:1216–1219.

Speakman, J. R. 2005. Body size, energy metabolism and lifespan. J. Exp. Biol. 208:1717–1730.

Springer, M., W. Murphy, E. Eizirik, and S. O'Brien. 2003. Placental mammal diversification and the Cretaceous–tertiary boundary. Proc. Natl. Acad. Sci. USA 100:1056–1061.

Springer, M. S., A. Burk-Herrick, R. Meredith, E. Eizirik, E. Teeling, S. J. O'Brien, and W. J. Murphy. 2007. The adequacy of morphology for reconstructing the early history of placental mammals. Syst. Biol. 56:673–684.

Stanley, S. M. 1973. An explanation for Cope's rule. Evolution 27:1–26. Available at http://www.jstor.org/stable/2407115.

Thewissen, J. G., E. M. Williams, L. J. Roe, and S. T. Hussain. 2001. Skeletons of terrestrial cetaceans and the relationship of whales to artiodactyls. Nature 413:277–281.

Thorne, J. L., H. Kishino, and I. S. Painter. 1998. Estimating the rate of evolution of the rate of molecular evolution. Mol. Biol. Evol. 15:1647–1657.

Webster, A. J., and A. Purvis. 2002. Testing the accuracy of methods for reconstructing ancestral states of continuous characters. Proc. Biol. Sci. 269:143–149.

Welch, J. J., O. R. P. Bininda Emonds, and L. Bromham. 2008. Correlates of substitution rate variation in mammalian protein-coding sequences. BMC Evol. Biol. 8:53.

Wong, F., C. Carter, and R. Kohn. 2003. Efficient estimation of covariance selection models. Biometrika 90:809–830.

Wray, G., J. Levinton, and L. Shapiro. 1996. Molecular evidence for deep precambrian divergences among metazoan phyla. Science 274:568–573.

Yang, Z., and B. Rannala. 1997. Bayesian phylogenetic inference using DNA sequences: a Markov chain Monte Carlo method. Mol. Biol. Evol. 14:717–724.

Yoder, A., and Z. Yang. 2000. Estimation of primate speciation dates using local molecular clocks. Mol. Biol. Evol. 17:1081–1090.

Zuckerkandl, E., and L. Pauling. 1962. Molecular disease, evolution and genetic heterogeneity. Pp. 189–225 *in* M. Kasha and B. Pullman, eds. Horizons in biochemistry. Academic Press, New York.

Associate Editor: A. Cutter

Supporting Information

The following supporting information is available for this article:

Table S1. Covariance analysis without human longevity, and rhino, whale and elephant body masses.

Table S2. Covariance analysis using life-history data not averaged over species of the same genus.

Table S3. Accession numbers of all sequences included in the multiple sequence alignment.

Table S4. Estimates (95% credibility intervals) of ancestral life-history traits for several ancestral nodes.

Figure S1. Joint reconstruction of divergence times and female maturity (in days).

Figure S2. Joint reconstruction of divergence times and longevity (in years).

Figure S3. Joint reconstruction of divergence times and adult body mass (in grams) under the uncorrelated model.

Figure S4. Posterior distribution on ancestral age at maturity for several ancestors.

Figure S5. Posterior distribution on ancestral longevity for several ancestors.

Figure S6. Joint reconstruction of divergence times and adult body mass (in grams) under the covariant model, without the upper constraint of 65 Myrs on cetartiodactyls.

Figure S7. Joint reconstruction of divergence times and adult body mass (in grams) under the covariant model, using a uniform prior on divergence times.

Figure S8. Estimates of log body size compared between (a) two runs under the diagonal model, using the calibrations of Springer et al, 2003, or Benton et al, 2009 (b) two runs under the covariant model, using the calibrations of Springer et al, 2003, or Benton et al, 2009, (c) the covariant and the diagonal models using the calibrations of Springer et al, 2003, (d) the covariant and the diagonal models using the calibrations of Benton et al, 2009.

Supporting Information may be found in the online version of this article.

Please note: Wiley-Blackwell is not responsible for the content or functionality of any supporting information supplied by the authors. Any queries (other than missing material) should be directed to the corresponding author for the article.